Environ. Sci. Technol. **2006**, *40,* 7717−7724

Quantum Chemical Calculations of Sulfate Adsorption at the Al- and Fe-(Hydr)oxide-H_2O Interface—Estimation of Gibbs Free Energies

KRISTIAN W. PAUL,*,† JAMES D. KUBICKI,‡ AND DONALD L. SPARKS†

Department of Plant and Soil Sciences, 152 Townsend Hall, University of Delaware, Newark, Delaware 19716, and Department of Geosciences and Earth and Environmental Systems Institute, The Pennsylvania State University, University Park, Pennsylvania 16802

Quantum chemical calculations were performed to estimate relative Gibbs free energies of sulfate adsorption on variably charged Al- and Fe-(hydr)oxide clusters. Inner-sphere bidentate bridging and monodentate adsorption were predicted to be exergonic on positively charged Al- and Fe-(hydr)oxides (ranging from −19 to −124 kJ mol^{-1}). However, inner-sphere and H-bonded adsorption on neutral Al- and Fe-(hydr)oxides was predicted to be endergonic (ranging from +5 to +61 kJ mol^{-1}). At the highest positive surface charge, bidentate bridging adsorption was most thermodynamically favorable. At intermediate positive surface charge, bidentate bridging and monodentate adsorption energies were equivalent on Al-(hydr)oxides; monodentate adsorption was more thermodynamically favorable on Fe-(hydr)oxides as compared with bidentate bridging adsorption. The predicted thermodynamic favorability of sulfate adsorption on Al- and Fe-(hydr)oxides was directly related to positive surface charge and indirectly related to the HO^-/SO_4^{2-} exchange stoichiometry, χ. Predicted Gibbs free energies of bidentate bridging and monodentate sulfate adsorption on an Fe-(hydr)oxide cluster (charge = +1, χ = 1) agreed reasonably well with published experimental estimates of sulfate adsorption on geothite (predicted values −34 and −52 kJ mol^{-1}, respectively, and experimental range −36 to −30 kJ mol^{-1}).

Introduction

The fate and transport of sulfate in soil and aquatic environments is predominantly regulated by sorption reactions with Al- and Fe-(hydr)oxides and clay minerals. Sulfur is an essential plant nutrient, but its availability depends on the extent of sulfate interaction with soil minerals. Sulfate leaching from forest soils enhances base cation transport. Leached base cations such as Ca^{2+} and Mg^{2+} are often replaced by Al^{3+} in regions affected by acid rain (*1*). In acid mine drainage (AMD), high concentrations of sulfate are regulated by sorption on Fe-(hydr)oxides (and sulfate mineral formation). Treatment of toxic metals in AMD typically involves pH regulation using alkaline agents (precipitate and immobilize metals). Unfortunately, alkaline treatment may promote leaching and transport of high concentrations of sulfate to aquatic resources (*2*). In excess of 250 mg L^{-1}, sulfate is a potential contaminant, and controlling its concentration post-treatment is crucial (*3*). Hence, understanding the mechanisms of sulfate sorption is of fundamental importance.

Sposito (*4*) suggested that sulfate exhibits intermediate ligand exchange behavior forming both outer- and inner-sphere adsorption complexes on Al- and Fe-(hydr)oxides. Sulfate adsorption is influenced, to a varying extent, by pH, ionic strength, hydration state, and mineral surface structure and charge. Numerous investigations using infrared spectroscopy have attempted to identify equilibrium sulfate adsorption complexes on variably hydrated Al- and Fe-(hydr)-oxides (*5*−*19*). Interpretations of experimental results vary widely, possibly a reflection of the intermediate adsorption behavior of sulfate. Monodentate, bidentate bridging, and tridentate complexes have been suggested. Results have shown the coexistence of outer- and inner-sphere sulfate and suggest that sulfate and bisulfate complexes coexist at low pH or under dehydrated conditions.

Despite the wealth of research describing equilibrium sulfate adsorption on Al- and Fe-(hydr)oxides, the literature is lacking in reaction mechanisms. Elucidation of reaction pathways, determination of activation barriers, identification of potential intermediates, and estimates of adsorption (desorption) energies are scant. This is due to sub-millisecond sorption reactions reaching steady-state before most spectroscopic measurements can be performed and to the many possible ligand exchange pathways (*20*). For example, a minimum of three reaction pathways exist for bidentate bridging sulfate adsorption as a function of pH (*20*). Thorough understanding of these reaction mechanisms helps improve predictive surface complexation models, oftentimes used to assess fate and transport of chemical species in the environment.

The objective of this investigation was to predict the thermodynamic favorability of potential reaction pathways for sulfate adsorption on variably charged Al- and Fe-(hydr)-oxides before modeling the reaction pathways themselves. To address this objective, quantum chemical calculations were performed to estimate relative Gibbs free energies of adsorption corresponding to potential reaction pathways suggested from experimental data. The overall goal is to subsequently elucidate activation barriers and rate constants of favorable reaction pathways. Theoretical predictions of the reaction kinetics will be particularly useful when collection of experimental data may not be feasible.

Materials and Methods

Calculations were performed with Gaussian 03 (*21*). Hybrid molecular orbital/density functional theory (MO/DFT) was employed using the Becke 3-parameter nonlocal exchange (*22*, *23*) and the Lee et al. (*24*) gradient-corrected correlation functionals (i.e., B3LYP). Calculations involving Al- and Fe-(hydr)oxide clusters were performed using restricted closed-shell and unrestricted open-shell formalisms, respectively. The high-spin state of Fe(III) (s = 5/2 for each Fe atom) was specified for Fe-containing clusters.

Selected stoichiometrically balanced equations were modeled to estimate relative Gibbs free energies of sulfate adsorption on variably charged Al- and Fe-(hydr)oxide

* Corresponding author phone: (302)831-2052; fax: (302)831-0605; e-mail: kpaul@udel.edu.
† University of Delaware.
‡ The Pennsylvania State University.

10.1021/es061139y CCC: $33.50
Published on Web 11/01/2006

$$SO_4^{2-}(H_2O)_9 + [Al_2(OH)_5(OH_2)_5{\cdot}(H_2O)_6]^+ \rightarrow Al_2(OH)_4(OH_2)_4SO_4{\cdot}(H_2O)_6 + OH^-(H_2O)_{10}$$

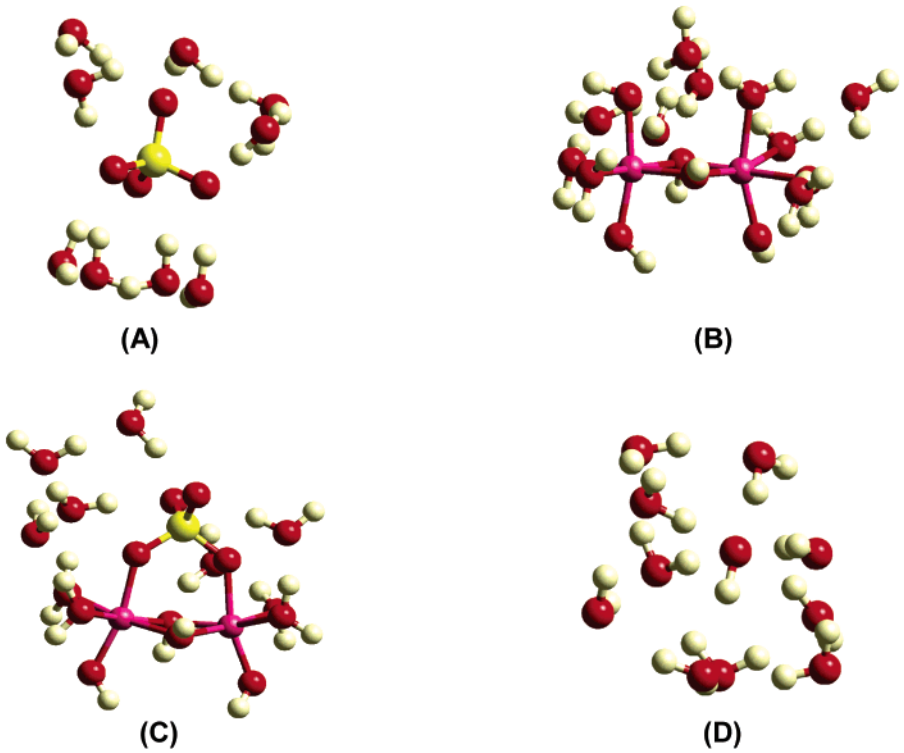

FIGURE 1. Example of a stoichiometrically balanced (mass and charge) reaction equation to estimate the Gibbs free energy of bidentate bridging adsorption for sulfate on a +1 charged Al-(hydr)oxide cluster. The ligand exchange reaction is characterized by sulfate replacing one H_2O and HO^- group ($\chi = 1$). (A) $SO_4^{2-}(H_2O)_9$ reactant. (B) $[Al_2(OH)_5(OH_2)_5{\cdot}(H_2O)_6]^+$ reactant. (C) $Al_2(OH)_4(OH_2)_4SO_4{\cdot}(H_2O)_6$ product. (D). $OH^-(H_2O)_{10}$ product. Oxygen (red); hydrogen (off-white); sulfur (yellow); and aluminum (pink).

clusters. Charges on each Al- and Fe-(hydr)oxide reactant were varied by adjusting the ratio of HO^-/H_2O functional groups terminating the models (i.e., changing the number of H^+ in the model). Charges on Al- and Fe-(hydr)oxide reactants ranged from +2 to 0. Sulfate adsorption was modeled for reactions occurring on surfaces at or below their pH_{pzc} (i.e., $pH \leq pH_{pzc}$, where pH_{pzc} is defined as the pH at which the net surface charge density equals zero (*25*)). Relative Gibbs free energies of sulfate adsorption were estimated for inner-sphere monodentate and bidentate bridging geometries and an outer-sphere H-bonded geometry.

To estimate relative Gibbs free energies of sulfate adsorption, model reactants and products were first geometry optimized without symmetry or geometrical constraints in the gas phase (e.g., Figure 1). Potential energy minima were verified by frequency calculations on the model structures (i.e., no imaginary frequencies). However, only one minimum was determined for each configuration, and the minima may not be global minima for these configurations (i.e., conformational analysis of potential energy surfaces not performed). Frequency calculations also determined the thermal corrections to Gibbs free energy (scaling not taken into account). Thermal correction to Gibbs free energy includes effects of molecular translation, rotation, and vibration at 298.15 K and 1.0 atm., as well as the zero-point vibrational energy (*26*).

For adsorption reactions involving Al-(hydr)oxide clusters, the all-electron 6-31+G(d,p) basis set was used to minimize the total electronic energy. Adsorption reactions involving Fe-(hydr)oxide clusters used a relativistic effective core potential (ECP) for the Fe atoms and the all-electron 6-31+G-(d,p) basis set for S, O, and H atoms to minimize the total electronic energy. The relativistic ECP used was the CEP-121G basis set (*27*). A comparison of the ECP and all-electron methods was conducted for one reaction to ensure consistent results. Use of relativistic ECPs with Hartree−Fock theory on Fe(III)-aquo ions has been shown to reduce basis set superposition error (*28*) and improves computational efficiency. The B3LYP/6-31+G(d) method was recently used to calculate (bi)sulfate infrared frequencies for adsorption complexes on similar Fe-(hydr)oxide clusters and was successfully compared with spectroscopic data (*11*). Several recent DFT investigations related to oxyanion adsorption on Al- and Fe-(hydr)oxides have also used similar (or identical) methods to successfully compare with experimental data (*29*−*34*). Hence, the B3LYP functional in combination with the 6-31+G(d,p) (and CEP-121G for clusters containing Fe) basis set was used in this investigation.

Single-point energy calculations were performed on each geometry optimized gas-phase species using the 6-311++G-(df,pd) basis set in combination with the Integral Equation Formalism Polarized Continuum Model (IEFPCM) (*35*). Use of the larger basis set provided more accurate estimation of model reaction energies (*26*). IEFPCM calculations provided an estimate of the total free energy in solution (including nonelectrostatic terms) for each geometry optimized model species. The dielectric constant of bulk water ($\epsilon = 78.4$) was used. Thus, both short-range explicit hydration (gas-phase calculation) and long-range implicit hydration (IEFPCM calculation) were considered to account for solvation.

Results and Discussion

Inner-sphere sulfate complexation occurs via ligand exchange with mineral surface functional groups (H_2O and HO^-) and is primarily a function of pH, surface charge, and structure. He et al. (*20*) and Rajan (*36*) proposed a bidentate bridging mechanism for sulfate adsorption whereby the type of

exchanged surface functional groups depended on pH. A simplified view of the ligand exchange mechanism suggests that at low pH, reactive surface groups are primarily protonated, and sulfate exchanges with two H_2O. At intermediate pH, a mixture of reactive surface groups coexist (H_2O and HO^-), and sulfate exchanges with one HO^- and one H_2O. At higher pH near pH_{pzc}, sulfate exchanges only with surface HO^- (*20*). The HO^-/SO_4^{2-} stoichiometry, χ, which ranges from 0 (low pH) to 2 (high pH), provides straightforward bookkeeping of possible ligand exchange pathways. The challenge to identify the most likely reaction pathways without knowledge of their thermodynamic favorability is clearly noted. Furthermore, these arguments neglect potential exchange of sulfate with surface H_2O at pH_{pzc}.

For many years, macroscopic measurements of $\chi > 0$ (at intermediate to high pH) were thought to provide evidence of inner-sphere sulfate adsorption, in contrast to outer-sphere adsorption (*20*). It was assumed that outer-sphere adsorption was an electrostatic attraction between positively charged surface site(s) and the negatively charged sulfate anion, without release of HO^- to solution. However, He et al. (*20*) demonstrated that HO^- release is not unequivocal evidence for inner-sphere adsorption. Outer-sphere adsorption may also result in HO^- release, measured as an increase in pH. At low pH, the outer-sphere sulfate may be described as an electrostatically bound ion pair, sulfate being attracted to one or more positively charged H_2O functional groups (*20*). At intermediate to high pH, H_2O near the mineral surface may dissociatively adsorb and protonate uncharged surface sites (H^+ consumption at surface and HO^- release into solution) in concert with outer-sphere complexation of sulfate. In this scenario, χ would be nonzero at intermediate to high pH and complicate interpretation of macroscopic pH measurements.

The dependence of sulfate adsorption on pH and surface charge alone creates a complicated network of potential reaction pathways (excluding effects of ionic strength, mineral surface structure, and competing ions). These complexities motivated this investigation to evaluate the thermodynamic favorability of potential sulfate adsorption pathways on variably charged Al- and Fe-(hydr)oxides. The objective was to compare the thermodynamic favorability of individual reaction pathways, ultimately leading to prediction of activation barriers and rate constants. Energies calculated for potential reactants and products permit estimation of relative Gibbs free energies for sulfate adsorption pathways on variably charged Al- and Fe-(hydr)oxides. Sulfate adsorption on variably charged Al-(hydr)oxides will be examined first.

Table 1 lists the reactants and products used to calculate the adsorption energies (Table 2). Although this methodology includes enthalpy and entropy terms, the calculated Gibbs free energies of adsorption (Tables 2 and 4) neglect configurational entropy (i.e., the position of the solute within the polarized continuum solvent cavity, expected to largely cancel out between similar species). The calculated ΔG_{ads} values are appropriately viewed relative to one another, rather than individually on an absolute scale. These quantum chemical calculations do not explicitly account for pH, but pH-dependent surface charge is modeled by changing the number of H^+ in model clusters to generate an approximate charge at a given pH. In this investigation, several combinations of cluster charge and χ were chosen to approximate real systems (*20*, *36*). Al- and Fe-(hydr)oxide reactants with charges greater than +2 were not modeled because they are considered unrealistic.

Four adsorption reactions were modeled for bidentate bridging sulfate on Al-(hydr)oxides, two corresponding to $\chi = 0$ (+2 and +1 Al-(hydr)oxide reactants) (Table 2). By way of an example, Figure 1 illustrates each reactant and product

TABLE 1. Reactant and Product Energies Calculated for Each Species in the Stoichiometrically Balanced (Mass and Charge) Equations to Approximate the Gibbs Free Energy of Sulfate Adsorption on Variably Charged Al-(Hydr)oxides[a]

Reaction Species	E_{gas}[b]	$E_{thermal}$[c]	E_{IEFPCM}[d]
	Aqueous Species		
$SO_4^{2-}\cdot(H_2O)_9$	−1387.222	0.189	−1387.788
$10H_2O$	−764.493	0.201	−764.762
$OH^-\cdot(H_2O)_9$	−763.959	0.190	−764.276
$OH^-\cdot(H_2O)_{10}$	−840.413	0.214	−840.751
$(OH^-)_2\cdot(H_2O)_9$	−839.767	0.199	−840.269
	Surface Clusters		
$[Al_2(OH)_4(OH_2)_6\cdot(H_2O)_6]^{2+}$	−1705.496	0.304	−1706.210
$[Al_2(OH)_5(OH_2)_5\cdot(H_2O)_6]^{+}$	−1705.199	0.291	−1705.746
$Al_2(OH)_6(OH_2)_4\cdot(H_2O)_6$	−1704.810	0.288	−1705.295
	Bidentate Bridging Complexes		
$Al_2(OH)_4(OH_2)_4SO_4\cdot(H_2O)_6$	−2252.225	0.273	−2252.809
$[Al_2(OH)_5(OH_2)_3SO_4\cdot(H_2O)_6]^-$	−2251.699	0.261	−2252.325
	Monodentate Complexes		
$Al_2(OH)_4(OH_2)_5SO_4\cdot(H_2O)_6$	−2328.659	0.300	−2329.270
$[Al_2(OH)_5(OH_2)_4SO_4\cdot(H_2O)_6]$[e]	−2328.152	0.286	−2328.798
$[Al_2(OH)_5(OH_2)_4SO_4\cdot(H_2O)_6]$[f]	−2328.141	0.286	−2328.787
	H-bonded Complex		
$Al_2(OH)_4(OH_2)_6SO_4\cdot(H_2O)_9$	−2634.475	0.391	−2635.186

[a] Energies are listed in Hartrees/molecule. [b] Gas-phase electronic energy of geometry optimized species (B3LYP/6-31+G(d,p)). [c] Thermal correction to Gibbs free energy. [d] Total free energy in solution with all nonelectrostatic terms from single-point energy calculations (B3LYP/6-311++G(df,pd)). [e] Monodentate sulfate H-bonded to a H_2O functional group occupying the next-nearest neighbor surface site. [f] Monodentate sulfate H-bonded to an OH functional group occupying the next-nearest neighbor surface site.

for bidentate bridging adsorption ($\chi = 1$; reactant surface charge = +1), corresponding to an adsorption energy of −47 kJ mol^{-1} (Table 2). Bidentate bridging reactions were predicted to be exergonic (−124 to −47 kJ mol^{-1}) on positively charged Al-(hydr)oxides (+2 and +1, $\chi = 0$ or 1), but endergonic (+6 kJ mol^{-1}) on a neutral Al-(hydr)oxide surface ($\chi = 2$) (Table 2). Note that an adsorption reaction involving a neutral Al-(hydr)oxide reactant and sulfate exchange with one H_2O and one HO^- ($\chi = 1$) is conceivable for bidentate bridging complexation (not listed in Tables 2 and 4). However, results in Table 1 (and Table 3) show this reaction to be endergonic. Thus, bidentate bridging adsorption on a neutral cluster was thermodynamically unfavorable, regardless of whether $\chi = 2$ or 1.

Five adsorption reactions were modeled for monodentate sulfate on Al-(hydr)oxides ($\chi = 0$ or 1) (Table 2). Similar to bidentate bridging adsorption, monodentate adsorption was exergonic (−66 to −19 kJ mol^{-1}) on positively charged Al-(hydr)oxides and endergonic (+22 to +52 kJ mol^{-1}) on neutral Al-(hydr)oxides. The influence of next-nearest neighbor surface sites (i.e., functional group type) on sulfate adsorption is not understood and has received little attention. Toward understanding this influence, monodentate adsorption energies were calculated for reactions on +1 and neutral Al-(hydr)oxides, where the next-nearest neighbor site was occupied by either an H_2O or HO^- functional group. Monodentate adsorption energies calculated for sulfate H-bonded with an HO^- functional group were significantly lower as compared to sulfate H-bonded with an H_2O functional group (Table 2). Sulfate interaction with a more labile group (H_2O) resulted in comparatively larger adsorption energies with respect to a less labile group (HO^-) (e.g., −48 vs −19 kJ mol^{-1} on +1 Al-(hydr)oxide reactant). Thus, lability of the surface functional group influenced the adsorption energies.

A series of H-bonded (outer-sphere) sulfate adsorption reactions were modeled (Table 2). As compared to inner-

TABLE 2. Estimated Gibbs Free Energies of Sulfate Adsorption on Variably Charged Al-(Hydr)oxides Using Calculated Values Listed in Table 1[a]

	bidentate bridging complexes
+2 cluster ($\chi = 0$)	$SO_4^{2-}(H_2O)_9 + [Al_2(OH)_4(OH_2)_6{\cdot}(H_2O)_6]^{2+} \rightarrow Al_2(OH)_4(OH_2)_4SO_4{\cdot}(H_2O)_6 + 1.1[10H_2O]$ $\Delta G = -124.0$
+1 cluster ($\chi = 0$)	$SO_4^{2-}(H_2O)_9 + [Al_2(OH)_5(OH_2)_5{\cdot}(H_2O)_6]^{+} \rightarrow [Al_2(OH)_5(OH_2)_3SO_4{\cdot}(H_2O)_6]^{-} + 1.1[10H_2O]$ $\Delta G = -70.4$
+1 cluster ($\chi = 1$)	$SO_4^{2-}(H_2O)_9 + [Al_2(OH)_5(OH_2)_5{\cdot}(H_2O)_6]^{+} \rightarrow Al_2(OH)_4(OH_2)_4SO_4{\cdot}(H_2O)_6 + OH^{-}(H_2O)_{10}$ $\Delta G = -47.2$
0 cluster ($\chi = 2$)	$SO_4^{2-}(H_2O)_9 + Al_2(OH)_6(OH_2)_4{\cdot}(H_2O)_6 \rightarrow Al_2(OH)_4(OH_2)_4SO_4{\cdot}(H_2O)_6 + (OH^{-})_2(H_2O)_9$ $\Delta G = +5.9$
	monodentate complexes
+2 cluster ($\chi = 0$)	$SO_4^{2-}(H_2O)_9 + [Al_2(OH)_4(OH_2)_6{\cdot}(H_2O)_6]^{2+} \rightarrow Al_2(OH)_4(OH_2)_5SO_4{\cdot}(H_2O)_6 + 10H_2O$ $\Delta G = -66.4$
+1 cluster ($\chi = 0$)	$SO_4^{2-}(H_2O)_9 + [Al_2(OH)_5(OH_2)_5{\cdot}(H_2O)_6]^{+} \rightarrow [Al_2(OH)_5(OH_2)_4SO_4{\cdot}(H_2O)_6]^{-} + 10H_2O$ $\Delta G = -48.1$[b]
+1 cluster ($\chi = 0$)	$SO_4^{2-}(H_2O)_9 + [Al_2(OH)_5(OH_2)_5{\cdot}(H_2O)_6]^{+} \rightarrow [Al_2(OH)_5(OH_2)_4SO_4{\cdot}(H_2O)_6]^{-} + 10H_2O$ $\Delta G = -18.8$[c]
0 cluster ($\chi = 1$)	$SO_4^{2-}(H_2O)_9 + Al_2(OH)_6(OH_2)_4{\cdot}(H_2O)_6 \rightarrow [Al_2(OH)_5(OH_2)_4SO_4{\cdot}(H_2O)_6]^{-} + OH^{-}(H_2O)_9$ $\Delta G = +22.2$[b]
0 cluster ($\chi = 1$)	$SO_4^{2-}(H_2O)_9 + Al_2(OH)_6(OH_2)_4{\cdot}(H_2O)_6 \rightarrow [Al_2(OH)_5(OH_2)_4SO_4{\cdot}(H_2O)_6]^{-} + OH^{-}(H_2O)_9$ $\Delta G = +51.5$[c]
	H-bonded complex
+2 cluster ($\chi = 0$)	$SO_4^{2-}(H_2O)_9 + [Al_2(OH)_4(OH_2)_6{\cdot}(H_2O)_6]^{2+} \rightarrow Al_2(OH)_4(OH_2)_6SO_4{\cdot}(H_2O)_9 + 6/10[10H_2O]$ $\Delta G = -68.8$
+1 cluster ($\chi = 1$)	$SO_4^{2-}(H_2O)_9 + [Al_2(OH)_5(OH_2)_5{\cdot}(H_2O)_6]^{+} + 10H_2O \rightarrow Al_2(OH)_4(OH_2)_6SO_4{\cdot}(H_2O)_9 + 6/10[10H_2O] + OH^{-}(H_2O)_9$ $\Delta G = -7.8$
0 cluster ($\chi = 2$)	$SO_4^{2-}(H_2O)_9 + Al_2(OH)_6(OH_2)_4{\cdot}(H_2O)_6 + 1.1[10H_2O] \rightarrow Al_2(OH)_4(OH_2)_6SO_4{\cdot}(H_2O)_9 + 6/10[10H_2O] + (OH^{-})_2(H_2O)_9$ $\Delta G = +61.2$

[a] Energies are listed in kJ mol^{-1} (1 Hartree = 2625.5 kJ mol^{-1}). [b] Monodentate sulfate H-bonded to a H_2O functional group occupying the next-nearest neighbor surface site. [c] Monodentate sulfate H-bonded to an OH functional group occupying the next-nearest neighbor surface site.

TABLE 3. Reactant and Product Energies Calculated for Each Species in the Stoichiometrically Balanced (Mass and Charge) Equations to Approximate the Gibbs Free Energy of Sulfate Adsorption on Variably Charged Fe-(Hydr)oxides[a]

Reaction Species	E_{gas}[b]	$E_{thermal}$[c]	E_{IEFPCM}[d]
	Surface Clusters		
$[Fe_2(OH)_4(OH_2)_6{\cdot}(H_2O)_6]^{2+}$	−1467.088	0.287	−1467.753
$[Fe_2(OH)_5(OH_2)_5{\cdot}(H_2O)_6]^{+}$	−1466.788	0.276	−1467.296
$Fe_2(OH)_6(OH_2)_4{\cdot}(H_2O)_6$	−1466.393	0.272	−1466.840
	Bidentate Bridging Complexes		
$Fe_2(OH)_4(OH_2)_4SO_4{\cdot}(H_2O)_6$	−2013.803	0.258	−2014.353
$[Fe_2(OH)_5(OH_2)_3SO_4{\cdot}(H_2O)_6]^{-}$	−2013.286	0.247	−2013.875
	Monodentate Complexes		
$Fe_2(OH)_4(OH_2)_5SO_4{\cdot}(H_2O)_6$	−2090.241	0.284	−2090.822
$[Fe_2(OH)_5(OH_2)_4SO_4{\cdot}(H_2O)_6]^{-}$[e]	−2089.741	0.273	−2090.351
	H-bonded Complex		
$Fe_2(OH)_4(OH_2)_6SO_4{\cdot}(H_2O)_9$	−2396.047	0.375	−2396.731

[a] Energies are listed in Hartrees/molecule. Some pertinent reactant species are listed in Table 1. [b] Gas-phase electronic energy of geometry optimized species (B3LYP/CEP-121G//6-31+G(d,p)). [c] Thermal correction to Gibbs free energy. [d] Total free energy in solution with all nonelectrostatic terms from single-point energy calculation (B3LYP/CEP-121G//6-311++G(df,pd)). [e] Monodentate sulfate H-bonded to a H_2O functional group occupying the next-nearest neighbor surface site.

sphere sulfate, H-bonded complexes were particularly challenging to model because they have more translational and rotational freedom. In this investigation, H-bonded sulfate similar to the geometry conceptualized by He et al. (*20*) was modeled. Figure 2 shows the geometry of H-bonded sulfate (explicit H_2O molecules omitted for visual aid). H-bonded sulfate adsorption was predicted to be energetically favorable (−69 kJ mol^{-1}) at high positive surface charge, but moderately favorable to highly unfavorable (−8 and +61 kJ mol^{-1}) at intermediate and zero net positive charge, respectively (Table 2). Thus, the thermodynamic favorability of H-bonded sulfate adsorption was directly related to positive surface charge and indirectly related to χ.

Figure 3 summarizes the relative Gibbs free energies of sulfate adsorption on Al- and Fe-(hydr)oxides (predictions from Tables 2 and 4). A few general observations are noted, momentarily concentrating on reactions involving Al-(hydr)-oxides. For sulfate adsorption occurring on +2 charged Al-(hydr)oxides, bidentate bridging adsorption was most thermodynamically favorable. Monodentate and H-bonded sulfate adsorption were predicted to have equivalent adsorption energies. All three adsorption reactions were predicted to be thermodynamically favorable. Sulfate adsorption on +1 charged Al-(hydr)oxides was characterized by equivalent adsorption energies for bidentate bridging and monodentate but only moderately favorable for H-bonded sulfate adsorption. All reactions occurring on a net neutral Al-(hydr)oxide reactant were predicted to be thermodynamically unfavorable.

Equilibrium adsorption of sulfate on Al-oxides (e.g., hydrous Al-oxide, gibbsite, bayerite) from experimental evidence is inconclusive and debated. Rajan (*36*) proposed bidentate bridging adsorption from surface charge measurements, in line with the comparatively high thermodynamic favorability of this complex (−124 vs −66 and −69 kJ mol^{-1} for monodentate and H-bonded sulfate on +2 Al-(hydr)-oxide, respectively; Table 2). Gessa et al. (*6*) also proposed bidentate bridging adsorption on dried amorphous aluminum hydroxide samples using IR spectroscopy. However, studies have shown that sulfate adsorption on Al-(hydr)-oxides may be characterized by outer-sphere (H-bonded) complexation and is sensitive to hydration (*13*, *17*). Hydration effects on sulfate adsorption energies determined via quantum chemical calculations were beyond the scope of this investigation. However, note from Figure 3 (Table 2) that both inner-sphere and H-bonded sulfate adsorption was

TABLE 4. Estimated Gibbs Free Energies of Sulfate Adsorption on Variably Charged Fe-(Hydr)oxides Using Calculated Values Listed in Table 3[a]

	bidentate bridging complexes
+2 cluster ($\chi = 0$)	$SO_4^{2-}(H_2O)_9 + [Fe_2(OH)_4(OH_2)_6{\cdot}(H_2O)_6]^{2+} \rightarrow Fe_2(OH)_4(OH_2)_4SO_4{\cdot}(H_2O)_6 + 1.1[10H_2O]$ $\Delta G = -122.8$
+1 cluster ($\chi = 0$)	$SO_4^{2-}(H_2O)_9 + [Fe_2(OH)_5(OH_2)_5{\cdot}(H_2O)_6]^{+} \rightarrow [Fe_2(OH)_5(OH_2)_3SO_4{\cdot}(H_2O)_6]^{-} + 1.1[10H_2O]$ $\Delta G = -67.2$
+1 cluster ($\chi = 1$)	$SO_4^{2-}(H_2O)_9 + [Fe_2(OH)_5(OH_2)_5{\cdot}(H_2O)_6]^{+} \rightarrow Fe_2(OH)_4(OH_2)_4SO_4{\cdot}(H_2O)_6 + OH^{-}(H_2O)_{10}$ $\Delta G = -33.6$
0 cluster ($\chi = 2$)	$SO_4^{2-}(H_2O)_9 + Fe_2(OH)_6(OH_2)_4{\cdot}(H_2O)_6 \rightarrow Fe_2(OH)_4(OH_2)_4SO_4{\cdot}(H_2O)_6 + (OH^{-})_2(H_2O)_9$ $\Delta G = +6.3$
	monodentate complexes
+2 cluster ($\chi = 0$)	$SO_4^{2-}(H_2O)_9 + [Fe_2(OH)_4(OH_2)_6{\cdot}(H_2O)_6]^{2+} \rightarrow Fe_2(OH)_4(OH_2)_5SO_4{\cdot}(H_2O)_6 + 10H_2O$ $\Delta G = -87.3$[b]
+2 cluster ($\chi = 0$)	$SO_4^{2-}(H_2O)_9 + [Fe_2(OH)_4(OH_2)_6{\cdot}(H_2O)_6]^{2+} \rightarrow Fe_2(OH)_4(OH_2)_5SO_4{\cdot}(H_2O)_6 + 10H_2O$ $\Delta G = -87.7$[c]
+1 cluster ($\chi = 0$)[b]	$SO_4^{2-}(H_2O)_9 + [Fe_2(OH)_5(OH_2)_5{\cdot}(H_2O)_6]^{+} \rightarrow Fe_2(OH)_5(OH_2)_4SO_4{\cdot}(H_2O)_6]^{-} + 10H_2O$ $\Delta G = -51.7$
0 cluster ($\chi = 1$)[c]	$SO_4^{2-}(H_2O)_9 + Fe_2(OH)_6(OH_2)_4{\cdot}(H_2O)_6 \rightarrow [Fe_2(OH)_5(OH_2)_4SO_4{\cdot}(H_2O)_6]^{-} + OH^{-}(H_2O)_9$ $\Delta G = +5.3$
	H-bonded complex
+2 cluster ($\chi = 0$)	$SO_4^{2-}(H_2O)_9 + [Fe_2(OH)_4(OH_2)_6{\cdot}(H_2O)_6]^{2+} \rightarrow Fe_2(OH)_4(OH_2)_6SO_4{\cdot}(H_2O)_9 + 6/10[10H_2O]$ $\Delta G = -71.3$
+1 cluster ($\chi = 1$)	$SO_4^{2-}(H_2O)_9 + [Fe_2(OH)_5(OH_2)_5{\cdot}(H_2O)_6]^{+} + 10H_2O \rightarrow Fe_2(OH)_4(OH_2)_6SO_4{\cdot}(H_2O)_9 + 6/10[10H_2O] + OH^{-}(H_2O)_9$ $\Delta G = +2.3$
0 cluster ($\chi = 2$)	$SO_4^{2-}(H_2O)_9 + Fe_2(OH)_6(OH_2)_4{\cdot}(H_2O)_6 + 1.1[10H_2O] \rightarrow Fe_2(OH)_4(OH_2)_6SO_4{\cdot}(H_2O)_9 + 6/10[10H_2O] + (OH^{-})_2(H_2O)_9$ $\Delta G = +57.9$

[a] Energies are listed in kJ mol^{-1} (1 Hartree = 2625.5 kJ mol^{-1}). [b] Geometry optimizations of Fe-containing species performed without use of a relativistic effective core potential basis set (B3LYP/6-31+G(d,p)). [c] Geometry optimizations of Fe-containing species performed with use of a relativistic effective core potential basis set in combination with all-electron basis set for the O, S, and H atoms (B3LYP/CEP-121G//6-31+G(d,p)).

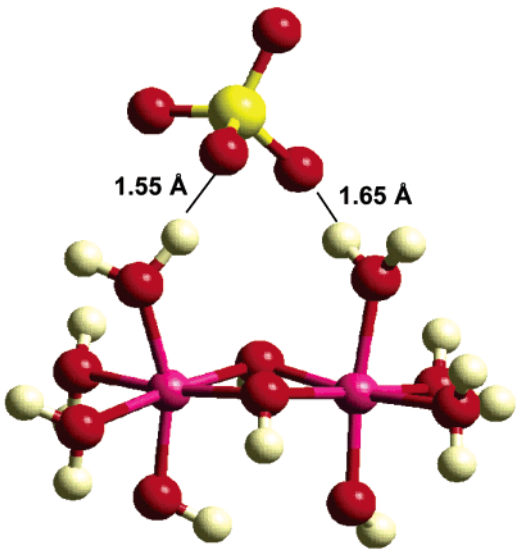

FIGURE 2. H-bonded sulfate adsorption product, $Al_2(OH)_4(OH_2)_6$-$SO_4{\cdot}(H_2O)_9$. The nine explicit H_2O molecules of hydration were omitted to simplify the figure and highlight H-bonding interactions with Al-(hydr)oxide surface H_2Os. Oxygen (red); hydrogen (off-white); sulfur (yellow); and aluminum (pink).

thermodynamically favorable at high to intermediate positive surface charge (+2 to +1).

A well established characteristic of sulfate adsorption on variably charged Al- and Fe-(hydr)oxides is the relationship between surface loading and equilibrium pH. Numerous macroscopic and spectroscopic results indicate that with increasing pH, sulfate adsorption sharply decreases on Al- and Fe-(hydr)oxides and soils (*12*, *15*, *17*, *20*, *36*–*47*). The inverse relationship between surface loading and pH is primarily attributed to a reduction in positively charged surface sites and increased competition with HO^- adsorption. Results presented here qualitatively agree with this experimental observation. Experimentally, sulfate adsorption generally does not occur at or above a mineral's bulk pH_{pzc}, where the net surface charge averaged over all the crystal faces is neutral. MO/DFT results correlate well with this observation in that adsorption reactions were predicted to be endergonic on net neutral reactant clusters (Figure 3). As the positive surface charge increases, the thermodynamic favorability of sulfate adsorption increases (Figure 3), which is expressed experimentally in the partition coefficient and equilibrium constant (*48*).

Table 3 lists the reactants and products used to calculate the adsorption energies for reactions involving Fe-(hydr)-oxides (Table 4). Two adsorption free energies were calculated for monodentate sulfate on the +2 Fe-(hydr)oxide: −87.7 and −87.3 kJ mol^{-1} (Table 4). These values corresponded to Gibbs free energies of sulfate adsorption with and without the use of a relativistic ECP on the Fe atoms, respectively. The energies were indistinguishable (i.e., equivalent optimized geometries), and thus, relativistic ECPs were used to minimize computational cost as compared to an all-electron basis set. To facilitate comparison between sulfate adsorption energies on Al- and Fe-(hydr)oxides, identical reactions were modeled (Tables 2 and 4). The exception was monodentate sulfate on Fe-(hydr)oxides, which only involved the next-nearest neighbor H_2O functional group.

The relative Gibbs free energies for bidentate bridging sulfate adsorption on Al- and Fe-(hydr)oxides were approximately equal and followed similar trends, particularly for reactants with +2 and 0 net surface charges (Figure 3). Similar adsorption energies for bidentate bridging sulfate on Al- and Fe-(hydr)oxides may correlate well with previous experimental results (*49*). Aylmore et al. (*49*) observed nearly identical adsorption−desorption isotherms for sulfate on hematite and pseudoboehmite, qualitative evidence for similar reaction mechanisms and energies. Furthermore, significant hysteresis between adsorption and desorption isotherms suggested an irreversible adsorption mechanism

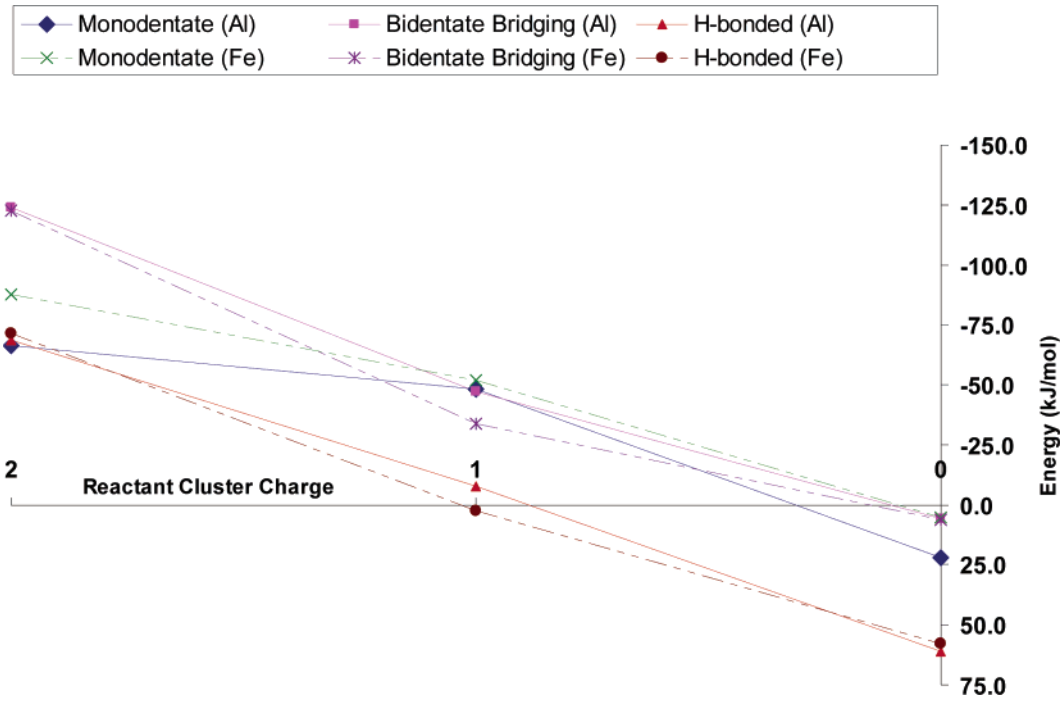

FIGURE 3. Estimation of Gibbs free energies of sulfate adsorption on variably charged Al- and Fe-(hydr)oxides. Values reported are from Tables 2 and 4. For monodentate sulfate complexes, plotted values correspond to next-nearest neighbor site occupied by a H_2O functional group. Bidentate bridging sulfate values plotted at $x = 1$ correspond to $\chi = 1$.

(*49*). As compared to monodentate or H-bonded adsorption, bidentate bridging sulfate adsorption should exhibit the largest degree of irreversibility (hysteresis) because two bonds must be broken prior to desorption. Figure 3 also shows that at highest positive surface charge, monodentate adsorption was more thermodynamically favorable on Fe-(hydr)oxides (−88 kJ mol^{-1}) as compared with Al-(hydr)oxides (−66 kJ mol^{-1}) (Tables 2 and 4). At intermediate surface charges, monodentate adsorption was thermodynamically equivalent on Al- and Fe-(hydr)oxides (−48 and −52 kJ mol^{-1}, respectively, $\chi = 0$) and slightly more exergonic than bidentate bridging adsorption (+1 reactants, $\chi = 1$) (Tables 2 and 4 and Figure 3).

The most commonly proposed adsorption geometry for sulfate on Fe-(hydr)oxides from spectroscopy has been bidentate bridging (*7*, *10*, *11*, *16*, *18*, *43*). Similar to sulfate adsorption on Al-(hydr)oxides (Table 2), bidentate bridging adsorption was estimated to be most thermodynamically favorable at the highest positive surface charge (Table 4 and Figure 3). However, the majority of these studies were conducted on variably hydrated/dehydrated samples, and some investigators have speculated and shown that sample dehydration may affect the equilibrium species or geometry (*8*, *11*, *12*). The effects of hydration on adsorption remain to be fully elucidated.

Hansmann and Anderson (*48*) used Stern theory as the basis for a statistical model to estimate the free energy of sulfate adsorption on goethite from electrophoretic measurements. The statistical model differed from surface complexation models because it was not constrained by a priori knowledge of the reaction stoichiometry. Measurements between pH 4 and 6 had corresponding net free energies of adsorption approximately equal to −36 and −30 kJ mol^{-1} ($\Delta G_{net} = \Delta G_{intrinsic} + \Delta G_{electrostatic}$). The experimental estimates agree reasonably well with MO/DFT calculated Gibbs free energies of adsorption for monodentate and bidentate bridging sulfate on Fe-(hydr)oxides possessing a net charge of +1 (Table 4, −52 and −34 kJ mol^{-1}, respectively). Infrared studies of sulfate adsorption on goethite (*12*, *17*) suggested monodentate complexation below pH 6. Several ex situ spectroscopic studies of sulfate adsorption on goethite have suggested bidentate bridging complexation (*9*, *10*, *18*, *43*). Setting aside the discrepancy regarding monodentate versus bidentate bridging adsorption on variably hydrated Fe-(hydr)oxides, the complementary nature of the MO/DFT calculations is demonstrated. Combining the experimental electrophoretic measurements (*48*), IR spectra, and MO/DFT Gibbs free energy calculations (Table 4), a more comprehensive picture of sulfate adsorption can be drawn.

Recently, flow adsorption calorimetry was used to determine arsenate sorption energies on amorphous Al-(hydr)oxide (*50*). Unfortunately, this technique is underutilized despite its potential to complement spectroscopy and quantum chemical calculations. Flow adsorption calorimetry measurements would be particularly helpful in testing the MO/DFT thermodynamic predictions. Calorimetric measurements could be informative with respect to the relevance of clusters in modeling actual surfaces of Al- and Fe-(hydr)oxides and potential mechanistic information predicted by the calculations. Future research could then focus on evaluating whether larger clusters or explicit treatment of additional water molecules would be necessary to improve the molecular modeling. Improvement of the molecular modeling may also arise from the choice of methodology (electron exchange and correlation functionals and basis sets), use of higher level ab initio methods, and periodic DFT calculations. Improvement to predicted thermodynamic quantities such as adsorption free energies is anticipated with ensemble average techniques (e.g., molecular dynamics and Monte Carlo).

Acknowledgments

K.W.P. appreciates financial support from a University of Delaware fellowship. This material is based upon work supported by the National Science Foundation under Grant No. EPS-0447610. G03 calculations were performed at the Delaware Biotechnology Institute, Bioinformatics Center, and the Center for Environmental Kinetics Analysis at The Pennsylvania State University. We are grateful to James A.

Dyer and Ryan Tappero for their critical reviews prior to publication. We greatly appreciate helpful contributions from three anonymous reviewers.

Supporting Information Available

Details regarding calculation of Gibbs free energy for a single complexation pathway involving geometry optimization (and frequency calculation) performed in the IEFPCM model and comparison to gas-phase prediction (followed by single-point IEFPCM calculation). This material is available free of charge via the Internet at http://pubs.acs.org.

Literature Cited

(1) Brady, N. C.; Weil, R. R. *The Nature and Properties of Soils*, 12th ed.; Prentice Hall: Upper Saddle River, NJ, 1999.

(2) Rose, S.; Elliott, W. C. The effects of pH regulation upon the release of sulfate from ferric precipitates formed in acid mine drainage. *Appl. Geochem.* **2000**, *15* (1), 27−34.

(3) Freeze, R. A.; Cherry, J. A. What has gone wrong? *Ground Water* **1989**, *27* (4), 458−464.

(4) Sposito, G. *The Surface Chemistry of Soils*; Oxford University Press: New York, 1984.

(5) Eggleston, C. M.; Hug, S.; Stumm, W.; Sulzberger, B.; Afonso, M. D. Surface complexation of sulfate by hematite surfaces: FTIR and STM observations. *Geochim. Cosmochim. Acta* **1998**, *62* (4), 585−593.

(6) Gessa, C.; Decherchi, M. L.; Melis, P.; Micera, G.; Erre, L. S. Anion-induced metal binding in amorphous aluminum hydroxide. *Colloids Surf.* **1984**, *11* (1−2), 109−117.

(7) Harrison, J. B.; Berkheiser, V. E. Anion interactions with freshly prepared hydrous iron-oxides. Clays *Clay Miner.* **1982**, *30* (2), 97−102.

(8) Hug, S. J. In situ Fourier transform infrared measurements of sulfate adsorption on hematite in aqueous solutions. *J. Colloid Interface Sci.* **1997**, *188* (2), 415−422.

(9) Parfitt, R. L.; Smart, R. S. C. IR spectra from binuclear bridging complexes of sulfate adsorbed on goethite (α-FeOOH). *J. Chem. Soc., Faraday Trans. 1* **1977**, *73*, 796−802.

(10) Parfitt, R. L.; Smart, R. S. C. Mechanism of sulfate adsorption on iron-oxides. Soil Sci. *Soc. Am. J.* **1978**, *42* (1), 48−50.

(11) Paul, K. W.; Borda, M. J.; Kubicki, J. D.; Sparks, D. L. Effect of dehydration on sulfate coordination and speciation at the Fe-(hydr)oxide−water interface: A molecular orbital/density functional theory and Fourier transform infrared spectroscopic investigation. *Langmuir* **2005**, *21* (24), 11071−11078.

(12) Peak, D.; Ford, R. G.; Sparks, D. L. An in situ ATR-FTIR investigation of sulfate bonding mechanisms on goethite. *J. Colloid Interface Sci.* **1999**, *218* (1), 289−299.

(13) Serna, C. J.; White, J. L.; Hem, S. L. Anion-aluminum hydroxide gel interactions. Soil Sci. *Soc. Am. J.* **1977**, *41* (5), 1009−1013.

(14) Spielbauer, D. Implementation of the scanning multichannel technique in Raman spectroscopy and the application for the characterization of oxides. *Appl. Spectrosc.* **1995**, *49* (5), 650−654.

(15) Turner, L. J.; Kramer, J. R. Irreversibility of sulfate sorption on goethite and hematite. *Water, Air, Soil Pollut.* **1992**, *63* (1−2), 23−32.

(16) Watanabe, H.; Gutleben, C. D.; Seto, J. Sulfate ions on the surface of maghemite and hematite. *Solid State Ionics* **1994**, *69* (1), 29−35.

(17) Wijnja, H.; Schulthess, C. P. Vibrational spectroscopy study of selenate and sulfate adsorption mechanisms on Fe- and Al-(hydr)oxide surfaces. *J. Colloid Interface Sci.* **2000**, *229* (1), 286−297.

(18) Turner, L. J.; Kramer, J. R. Sulfate ion binding on goethite and hematite. *Soil Sci.* **1991**, *152* (3), 226−230.

(19) Persson, P.; Lovgren, L. Potentiometric and spectroscopic studies of sulfate complexation at the goethite−water interface. *Geochim. Cosmochim. Acta* **1996**, *60* (15), 2789−2799.

(20) He, L. M.; Zelazny, L. W.; Baligar, V. C.; Ritchey, K. D.; Martens, D. C. Hydroxyl-sulfate exchange stoichiometry on γ-Al_2O_3 and kaolinite. *Soil Sci. Soc. Am. J.* **1996**, *60* (2), 442−452.

(21) Frisch, M. J. et al. *Gaussian* 03; Gaussian, Inc.: Pittsburgh, PA, 2004.

(22) Stephens, P. J.; Devlin, F. J.; Chabalowski, C. F.; Frisch, M. J. Ab initio calculation of vibrational absorption and circular dichroism spectra using density-functional force-fields. *J. Phys. Chem.* **1994**, *98* (45), 11623−11627.

(23) Becke, A. D. Density-functional thermochemistry. 3. The role of exact exchange. J. *Chem. Phys.* **1993**, *98* (7), 5648−5652.

(24) Lee, C. T.; Yang, W. T.; Parr, R. G. Development of the Colle−Salvetti correlation energy formula into a functional of the electron density. *Phys. Rev. B* **1988**, *37* (2), 785−789.

(25) Sposito, G. On points of zero charge. *Environ. Sci. Technol.* **1998**, *32* (19), 2815−2819.

(26) Foresman, J. B.; Frisch, A. *Exploring chemistry with electronic structure methods*, 2nd ed.; Gaussian, Inc.: Pittsburgh, PA, 1996.

(27) Stevens, W. J.; Krauss, M.; Basch, H.; Jasien, P. G. Relativistic compact effective potentials and efficient, shared-exponent basis sets for the third row, fourth row, and fifth row atoms. *Can. J. Chem.* **1992**, *70* (2), 612−630.

(28) Rotzinger, F. P. Performance of molecular orbital methods and density functional theory in the computation of geometries and energies of metal aqua ions. *J. Phys. Chem. B* **2005**, *109* (4), 1510−1527.

(29) Bargar, J. R.; Kubicki, J. D.; Reitmeyer, R.; Davis, J. A. ATR-FTIR spectroscopic characterization of coexisting carbonate surface complexes on hematite. *Geochim. Cosmochim. Acta* **2005**, *69* (6), 1527−1542.

(30) Kwon, K. D.; Kubicki, J. D. Molecular orbital theory study on surface complex structures of phosphates to iron hydroxides: Calculation of vibrational frequencies and adsorption energies. *Langmuir* **2004**, *20* (21), 9249−9254.

(31) Ladeira, A. C. Q.; Ciminelli, V. S. T.; Duarte, H. A.; Alves, M. C. M.; Ramos, A. Y. Mechanism of anion retention from EXAFS and density functional calculations: Arsenic (V) adsorbed on gibbsite. *Geochim. Cosmochim. Acta* **2001**, *65* (8), 1211−1217.

(32) Sherman, D. M.; Randall, S. R. Surface complexation of arsenic (V) to iron (III) (hydr)oxides: Structural mechanism from ab initio molecular geometries and EXAFS spectroscopy. *Geochim. Cosmochim. Acta* **2003**, *67* (22), 4223−4230.

(33) Zhang, N. L.; Blowers, P.; Farrell, J. Evaluation of density functional theory methods for studying chemisorption of arsenite on ferric hydroxides. *Environ. Sci. Technol.* **2005**, *39* (13), 4816−4822.

(34) Tribe, L.; Kwon, K. D.; Trout, C. C.; Kubicki, J. D. Molecular orbital theory study on surface complex structures of glyphosate on goethite: Calculation of vibrational frequencies. *Environ. Sci. Technol.* **2006**, *40* (12), 3836−3841.

(35) Cances, E.; Mennucci, B.; Tomasi, J. A new integral equation formalism for the polarizable continuum model: Theoretical background and applications to isotropic and anisotropic dielectrics. *J. Chem. Phys.* **1997**, *107* (8), 3032−3041.

(36) Rajan, S. S. S. Sulfate adsorbed on hydrous alumina, ligands displaced, and changes in surface charge. Soil Sci. Soc. Am. J. **1978**, *42* (1), 39−44.

(37) Ali, M. A.; Dzombak, D. A. Competitive sorption of simple organic acids and sulfate on goethite. *Environ. Sci. Technol.* **1996**, *30* (4), 1061−1071.

(38) Courchesne, F. Electrolyte concentration and composition effects on sulfate sorption by two spodosols. Soil Sci. Soc. Am. J. **1991**, *55* (6), 1576−1581.

(39) Geelhoed, J. S.; Hiemstra, T.; VanRiemsdijk, W. H. Phosphate and sulfate adsorption on goethite: Single anion and competitive adsorption. *Geochim. Cosmochim. Acta* **1997**, *61* (12), 2389−2396.

(40) Gobran, G. R.; Selim, H. M.; Hultberg, H.; Andersson, I. Sulfate adsorption−desorption in a Swedish forest soil. *Water, Air, Soil Pollut.* **1998**, *108* (3−4), 411−424.

(41) Gustafsson, J. P. Modeling pH-dependent sulfate adsorption in the Bs horizons of podzolized soils. *J. Environ. Qual.* **1995**, *24* (5), 882−888.

(42) Marsh, K. B.; Tillman, R. W.; Syers, J. K. Charge relationships of sulfate sorption by soils. Soil Sci. *Soc. Am. J.* **1987**, *51* (2), 318−323.

(43) Martin, R. R.; Smart, R. S. X-Ray photoelectron studies of anion adsorption on goethite. Soil Sci. *Soc. Am. J.* **1987**, *51* (1), 54−56.

(44) Rose, S.; Ghazi, A. M. Release of sorbed sulfate from iron oxyhydroxides precipitated from acid mine drainage associated with coal mining. *Environ. Sci. Technol.* **1997**, *31* (7), 2136−2140.

(45) Sigg, L.; Stumm, W. The interaction of anions and weak acids with the hydrous goethite (α-FeOOH) surface. *Colloids Surf.* **1981**, *2* (2), 101−117.

(46) Singh, B. R. Sulfate sorption by acid forest soils. 3. Desorption of sulfate from adsorbed surfaces as a function of time, desorbing ion, pH, and amount of adsorption. *Soil Sci.* **1984**, *138* (5), 346−353.

(47) Zhang, P. C.; Sparks, D. L. Kinetics and mechanisms of sulfate adsorption/desorption on goethite using pressure-jump relaxation. *Soil Sci. Soc. Am. J.* **1990**, *54* (5), 1266−1273.
(48) Hansmann, D. D.; Anderson, M. A. Using electrophoresis in modeling sulfate, selenite, and phosphate adsorption onto goethite. *Environ. Sci. Technol.* **1985**, *19* (6), 544−551.
(49) Aylmore, L. A. G.; Karim, M.; Quirk, J. P. Adsorption and desorption of sulfate ions by soil constituents. *Soil Sci.* **1967**, *103* (1), 10−15.
(50) Kabengi, N. J.; Daroub, S. H.; Rhue, R. D. Energetics of arsenate sorption on amorphous aluminum hydroxides studied using flow adsorption calorimetry. *J. Colloid Interface Sci.* **2006**, *297* (1), 86−94.

Received for review May 12, 2006. Revised manuscript received August 4, 2006. Accepted August 15, 2006.

ES061139Y